Terahertz Waves Emitted from an Optical Fiber

Minwoo Yi,[1] Kanghee Lee,[1] Jongseok Lim,[1] Youngbin Hong,[2] Young-Dahl Jho,[2] and Jaewook Ahn[1,*]

[1]*Department of Physics, Korea Advanced Institute of Science and Technology, Daejeon 305-701 Korea*

[2]*Department of Information and Communication, Gwangju Institute of Science and Technology, Gwangju 500-712 Korea*

[*]*jwahn@kaist.ac.kr*

Abstract: We report a simple method of creating terahertz waves by applying the photo-Dember effect in a (100)-oriented InAs film coated onto the 45-degree wedged-end facet of an optical fiber. The terahertz waves are generated by infrared pulses guided through the optical fiber which is nearly in contact with a sample and then measured by a conventional photo-conductive antenna detector. Using this alignment-free terahertz source, we performed proof-of-principle experiments of terahertz time-domain spectroscopy and near-field terahertz microscopy. We obtained a bandwidth of 2 THz and 180-μm spatial resolution. Using this method, the THz imaging resolution is expected to be reduced to the size of the optical fiber core. Applications of this device can be extended to sub-wavelength terahertz spectroscopic imaging, miniaturized terahertz system design, and remote sensing.

OCIS codes: (300.6495) terahertz spectroscopy; (060.2380) Fiber optics sources and detectors

References and links

1. M. Tonouchi, "Cutting-edge terahertz technology," Nature Photonics **1**, 97-105 (2007).
2. J. S. Melinger, N. Laman, S. S. Harsha, and D. Grischkowsky, "Line narrowing of THz vibrational modes for organic thin films within a parallel plate waveguide," Appl. Phys. Lett. **89**, 251110 (2006).
3. H.-T. Chen, W. J. Padilla, J. M. O. Zide, A. C. Gossard, A. J. Taylor, and R. D. Averitt, "Active terahertz metamaterial devices," Nature **444**, 597-600 (2006).
4. X. Wang, A. A. Belyanin, S. A. Crooker, D. M. Mittleman, and J. Kono, "Interference-induced terahertz transparency in a semiconductor magneto-plasma," Nature Physics **6**, 126-130 (2010).
5. Q. Chen, Z. Jiang, G. X. Xu, and X.-C. Zhang, "Near-field terahertz imaging with a dynamic aperture," Opt. Lett. **25**, 1122-1124 (2000).
6. H. T. Chen, R. Kersting, and G. C. Cho, "Terahertz imaging with nanometer resolution," Appl. Phys. Lett. **83**, 3009-3011 (2003).
7. A. J. L. Adam, N. C. J. Van der Valk, and P. C. M. Planken, "Measurement and calculation of the near field of a terahertz apertureless scanning optical microscope," J. Opt. Soc. Am. B **24**, 1080-1090 (2007).
8. R. Lecaque, S. Gresillon, and C. Boccara, "THz emission Microscopy with sub-wavelength broadband source," Opt. Express **16**, 4731-4738 (2008).
9. M. Wachter, M. Nagel, and H. Kurz, "Tapered photoconductive terahertz field probe tip with subwavelength spatial resolution," Appl. Phys. Lett. **95**, 041112 (2009).
10. J. Bromage, S. Radic, G. P. Agrawal, C. R. Stroud, P. M. Fauchet, and R. Sobolewski, "Spatiotemporal shaping of half-cycle terahertz pulses by diffraction through conductive apertures of finite thickness," J. Opt. Soc. Am. B **15**, 1399-1405 (1988).
11. N. C. J. van der Valk and P. C. M. Planken, "Electro-optic detection of subwavelength terahertz spot sizes in the near field of a metal tip," Appl. Phys. Lett. **81**, 1558-1560 (2002).

#127512 - $15.00 USD Received 27 Apr 2010; revised 6 Jun 2010; accepted 7 Jun 2010; published 10 Jun 2010

12. M. Awad, M. Nagel, and H. Kurz, "Tapered Sommerfeld wire terahertz near-field imaging," Appl. Phys. Lett. **94**, 051107 (2009).
13. K. Wang and D. M. Mittleman, "Metal wires for terahertz wave guiding," Nature **432**, 376-379 (2004).
14. A. Bingham, Y. Zhao, and D. Grischkowsky, "THz parallel plate photonic waveguides," Appl. Phys. Lett. **87**, 051101 (2005).
15. S. P. Jamison, R.W. McGowan, and D. Grischkowsky, "Single-mode waveguide propagation and reshaping of sub-ps terahertz pulses in sapphire fibers," Appl. Phys. Lett. **76**, 1987-1989 (2000).
16. L.-J. Chen, H.-W. Chen, T.-F. Kao, J.-Y. Lu, and C.-K. Sun, "Low-loss subwavelength plastic fiber for terahertz waveguiding," Opt. Lett. **31**, 308-310 (2006).
17. T.-I. Jeon, and D. Grischkowsky, "Direct optoelectronic generation and detection of sub-ps-electrical pulses on sub-mm-coaxial transmission lines," Appl. Phys. Lett. **85**, 6092-6094 (2004).
18. M. Mbonye, R. Mendis, and D. M. Mittleman, "A terahertz two-wire waveguide with low bending loss," Appl. Phys. Lett. **95**, 233506 (2009).
19. S. A. Crooker, "Fiber-coupled antennas for ultrafast coherent terahertz spectroscopy in low temperatures and high magnetic fields," Rev. Sci. Instrum. **73**, 3258-3264 (2002).
20. K. Liu, J. Xu, T. Yuan, and X.-C. Zhang, "Terahertz radiation from InAs induced by carrier diffusion and drift," Phys. Rev. B **73**, 155330 (2006).
21. R. Inoue, K. Takayama, M. Tonouchi, "Angluar dependence of terahertz emission from semiconductor surfaces photoexcited by femtosecond optical pulses," J. Opt. Soc. Am. B **26** A14-A22 (2009).
22. P. Gu, M. Tani, S. Kono, K. Sakai, and X.-C. Zhang, "Study of terahertz radiation from InAs and InSb," J. Appl. Phys. **91**, 5533-5537 (2002).
23. R. Adomavičius, A. Urbanowicz, G. Molis, A. Krotkus, and E. Šatkovskis, "Terahertz emission from p-lnAs due to the instantaneous polarization," Appl. Phys. Lett. **85**, 2463-2465 (2004).

1. Introduction

Electromagnetic radiation at terahertz (THz) frequencies allows the visualization of many heretofore unobserved material properties associated with molecular responses to THz waves [1]. Technological advances in the THz region have already made possible the development of spectroscopic imaging systems to obtain spatially and temporally resolvable sample information by tracing the collective vibration modes of organic molecules [2], the structural resonances of semiconductors and metals [3], and even the oscillations of gaseous and solid-state plasmas [4]. The major technical obstacles for most THz imaging applications are absorption loss by water vapor, the difficulty in miniaturizing the system size, and the rather poorer imaging resolution than in the conventional spectral region.

In a generic THz imaging system based on passive optical components such as lenses and/or parabolic mirrors, the spatial image resolution is diffraction-limited to a few hundred microns. To overcome the diffraction limit, that is, to obtain a THz image of sub-wavelength scale, scanning near-field microscope techniques, also known as THz-SNOM, have been used [5, 6, 7, 8, 9]. The resolution is then not limited by the wavelength of the illuminating electromagnetic source, but rather by geometrical parameters such as the size of an aperture or a scatterer. However, in a THz-SNOM the detected THz signal is small and bandwidth-limited [6, 10]. Many attempts have been made to improve the signal-to-noise ratio and also the bandwidth of the THz signal [9, 11]; one alternative approach is guiding the THz wave through a probing tip [12].

However, the low coupling efficiency and radial distribution of the guided THz signal make finding an easy-to-use application of this method difficult. Sending THz waves through an elongated object, or THz waveguide, has been studied with metal wires [13], plates [14], and fibers [15, 16], and cables [17]. Even in those studies, because of attenuation and the bending losses, most of these waveguide methods are not viable in THz near-field spectroscopy and imaging [18]. The alternative is to generate and capture the THz signal near the sample by using an optical-fiber-coupled infrared (IR) pulse [19].

In this letter, we describe an idea for emitting THz waves directly from a conventional optical fiber as shown in Fig. 1(a). The end facet of the optical fiber is polished at an angle and coated

#127512 - $15.00 USD Received 27 Apr 2010; revised 6 Jun 2010; accepted 7 Jun 2010; published 10 Jun 2010

with an InAs thin film. An intense-field-density laser beam, guided through the optical fiber core, illuminates the InAs film and generates the THz waves. In a proof-of-principle experiment using the alignment-free THz source, we perform THz time-domain spectroscopy (THz-TDS) and near-field THz microscopy.

2. Experimental description

The THz waves were generated using the photo-Dember effect, or electric dipole formation near the surface of a semiconducting material, during ultrafast photo-absorption [20]. The mobility difference between electrons and holes forms an effective charge separation along the surface normal. The maximum THz emission in the reflection geometry under a focusing condition of the excitation beam is along broadly 45 degree from the InAs surface normal [21]. The optical fiber tip was therefore cut at an angle of 45 degrees to generate THz waves transmissively along the optical beam direction; see Fig. 1(b). The photo-Dember effect is relatively strong in narrow-band gap III-V semiconductors with high electron mobility, such as InAs and InSb, and therefore, they emit THz waves at an order of intensity magnitude higher than those of relatively wide band-gap semiconductors such as InP and GaAs [22]. By using the intrinsic mobility of InAs (30,000 $cm^2/(V \cdot s)$), the excess energy (1.2 eV from a 1.55-eV photon) at room temperature, and the momentum relaxation time of 500 fs, the diffusion length is estimated as 1.3 μm. Considering the THz absorption and effective Dember charge separation, we estimated

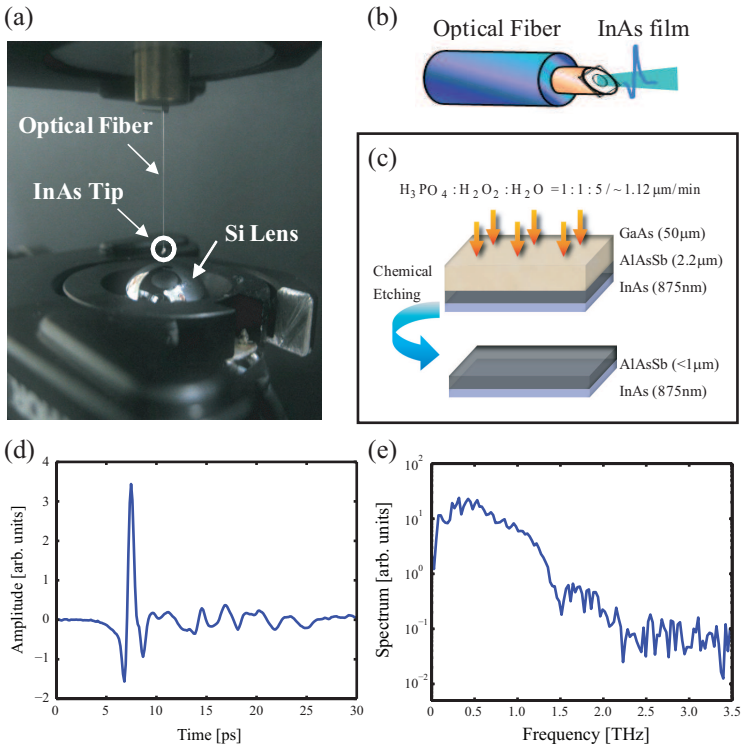

Fig. 1. (Color online) (a) Setup photograph of the THz optical fiber tip in a near-field microscope application. (b) Schematic of the optical fiber THz emitter. (c) InAs film fabrication layout. (d) Measured THz waveform from the optical-fiber THz emitter. (e) The amplitude spectrum of the THz pulse shown in (d).

#127512 - $15.00 USD Received 27 Apr 2010; revised 6 Jun 2010; accepted 7 Jun 2010; published 10 Jun 2010

that a 1-μm-thick InAs film would be optimal.

The (100)-oriented InAs thin film was grown using molecular beam epitaxy on AlAsSb-buffered semi-insulating GaAs (SI-GaAs) substrates. The AlAsSb buffer and the grown InAs film thicknesses were 2.2 μm and 875 nm, respectively. The SI-GaAs substrate is eliminated by lapping and chemical etching. The wet chemical etch process is enhanced by a phosphoric acid solution etchant ($H_3PO_4 : H_2O_2 : H_2O = 1 : 1 : 5$) with an etch rate of $\sim$1.12 μm/min. The wet chemical etching layout for the InAs thin film is shown in Fig. 1(c). The InAs film was cut down to the size of the fiber facet and then glued to the optical fiber tip with optical epoxy.

In order to test the THz emission of this device, we used 1.55-eV photons in a 70-fs ultrashort pulse train produced in a Ti:sapphire laser oscillator at a repetition rate of 90-MHz. For the generation and optically-gated detection of the THz waves, the laser pulses were physically separated by a beam splitter and temporally by a variable delay line. The optically pumped beam for the THz generation was then coupled to a 50-μm core diameter optical fiber. The 10-mW average laser pulses were then guided through a 20-cm-long optical fiber without dispersion compensation. The THz pulses radiated from the InAs thin film fixed on the polished optical fiber tip were detected by a conventional photoconductive antenna (PCA). The time-delayed probe beam was focused on the PCA through a silicon lens for temporal gating. Although the silicon lens in front of the PCA is assembled to optimally detect collimated incident THz waves, the fastly diverging THz signal emitted from the constructed fiber tip was readily detected in the experiment. The photo-current measured from the PCA was proportional to the generated THz electric field amplitude. The measured THz temporal signal and its amplitude spectrum from the conceived THz emitter are shown in Figs. 1(d) and (e). The measured spectral bandwidth is nearly 2 THz.

3. Results and discussions

The mechanism of THz generation from InAs can be both optical rectification and photo-Dember effect. Especially the THz waves from the optical rectification process has THz amplitude dependence on the polarization state of the pump beam. In our design of optical fiber THz emitters, we have used (100)-oriented InAs from which the THz emission is dominated by the photo-Dember effect [20]. Upon the pump beam incident being on the InAs surface, the gradient of the photo-excited electrons and holes is created due to the diffusion velocity mismatch between the electrons and holes. Then, the resulting photo-Dember current is polarized perpendicularly to the surface, and the generated THz pulse is p-polarized. Figure 2 shows the azimuthally angle-dependent amplitude of THz temporal waveforms measured as the optical fiber was rotated around the optical axis. The PCA detector recorded the horizontal polarization component of the THz waveforms as a function of time. The THz signals detected at three different times in Fig. 2(a) show the sinusoidal pattern around the optical axis, as shown in Fig. 2(b). This measurement shows that the measured THz signal is linearly polarized, as expected in THz generation process from the photo-Dember effect [23].

The 50-μm core diameter of the optical fiber was chosen because of the compatibility between generated THz power and resolution, which are simultaneously dependent on the core diameter. Figure 3(a) shows the dependence of the measured THz power on the incident optical power from the devised 50-μm core diameter THz emitter (star) and the bare InAs film on the 500-μm-thick sapphire substrate (solid lines). If a larger InAs area is excited by a given optical pulse under the saturation regime, greater THz power is obtained due to the increased induced photo-Dember field area. However, as the core size is increased, the resolution worsens because it relies on the size of the optical-fiber core. Therefore, to select the core diameter, we studied the dependence of the generated THz power on the optical beam diameter and incident optical power, which was applied to the sapphire substrate side. Two regimes must be dealt with:

#127512 - $15.00 USD Received 27 Apr 2010; revised 6 Jun 2010; accepted 7 Jun 2010; published 10 Jun 2010

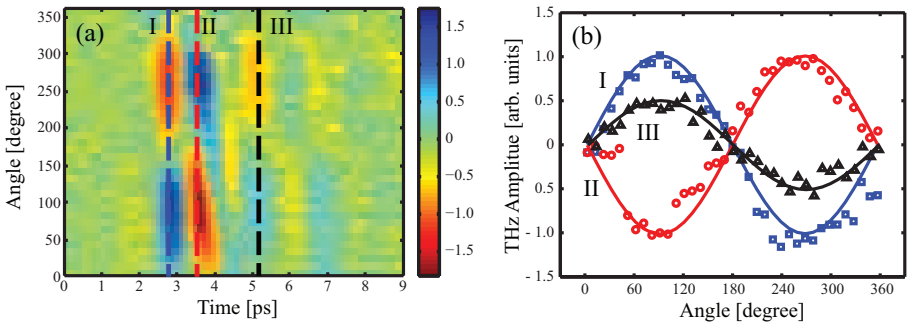

Fig. 2. (Color online) (a) Image of measured horizontal components of the THz field emitted from the fiber tip as a function of rotation angle and time. (b) The sinusoidal angle dependence around the optical axis at three different times (dashed line) shown in (a).

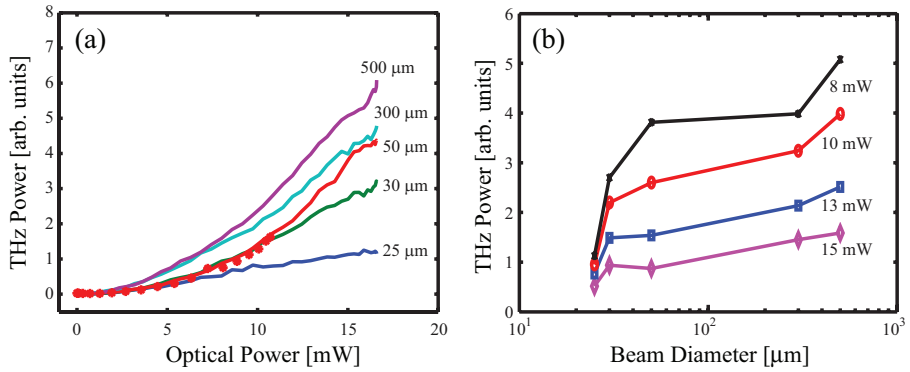

Fig. 3. (Color online) (a) Optical power dependence of the measured THz pulses from the devised optical-fiber THz emitter (star) and from a bare InAs film attached to a 500-μm-thick sapphire substrate (solid line). (b) Beam diameter dependence on the THz power from the bare InAs film.

$D \geq \lambda_{THz}$, and $D \ll \lambda_{THz}$, where D is the diameter of the optical beam and λ_{THz} is the typical wavelength of a THz pulse. From the results shown in the Fig. 3(b), we anticipate comparatively greater THz power with sub-wavelength resolution when the optical beam diameter has a 50-μm core fiber for $D \ll \lambda_{THz}$.

The spatial resolution of the THz emission fiber tip is demonstrated using a knife-edge method. The image target is an 18-μm-thick aluminum foil, placed at the distance of 100 μm from the optical fiber core. This distance is due to the 45-degree-cut angle of the optical fiber tip and the width of the fiber cladding. Keeping the relative time fixed at the THz pulse peak, we measured the THz amplitude using a 4-f conventional THz-TDS system. Figures 4 (a) and (b) depict a knife-edge imaging. The edge of the foil was moved from left to right, and an area of 400 $\times$ 200 μm^2 was scanned. The resolution of the microscope tip is measured 180 μm, defined by the 10-90 % criteria from the lateral profile taken from the line as drawn in the image in Fig. 4(a). This resolution is three times bigger than the size of the fiber core diameter, because of the positional departure of the sample from the tip due to the slanted end facet of the fiber and the thickness of the optical epoxy and InAs film.

For a near-field imaging proof-of-principle experiment, a metal sieve pattern of sub-wavelength dimension (200 $\times$ 200 μm^2 area open squares with 100-μm-wide metal wires)

#127512 - $15.00 USD Received 27 Apr 2010; revised 6 Jun 2010; accepted 7 Jun 2010; published 10 Jun 2010

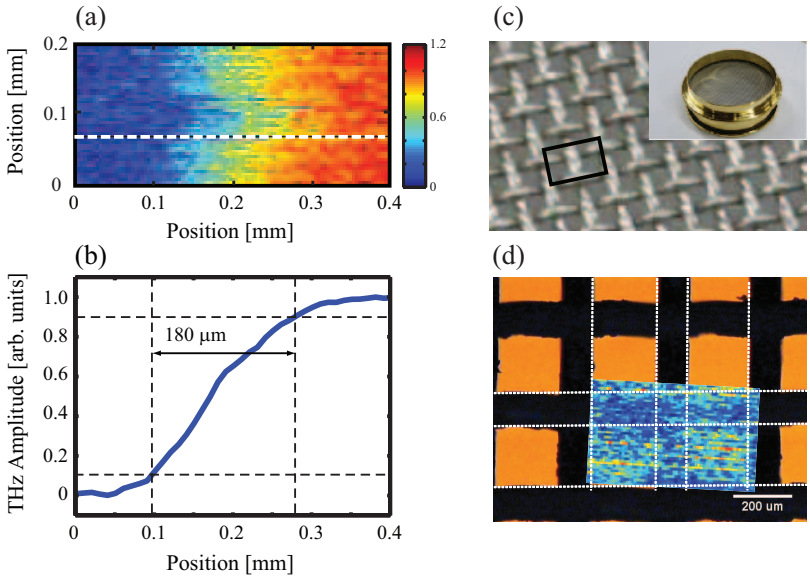

Fig. 4. (Color online) (a) A knife-edge THz image using an 18-μm-thick aluminum foil. (b) The lateral profile taken from a line as drawn in (a). (c) Optically magnified photo of the metal sieve and an overall view (inset). (d) THz image of (c) superimposed on an optical microscope image.

was measured. The optical image of the metal sieve is shown in Fig. 4(c), and the result is shown in (d). A THz-emission microscope-tip image of this sieve, superimposed on an optical-microscope image, is shown in Fig. 4(d). The spatially resolved THz-field image shows the pattern of the metal sieve. The 100-μm-wide metal wire lines and the open square area are apparently resolved. The slight blurring of the scanned image is attributed to the presence of the weaved shape in the real object as well as the distance between the source and the object. The distance between the fiber tip and the metal mesh was about 150-μm because of the tilted tip and cladding of the optical fiber. Using this method, the THz imaging resolution is expected to be reduced to the size of the optical fiber core.

Using this method, the size of this THz emitter may be reduced to the size of an optical fiber core, 1000 times smaller than previously considered PCA-based optical fiber THz emitters. Furthermore, the fabrication of this kind of THz emitters is nearly a material coating process, not a device assembly. This type of THz fiber emitters can be used as a topographical scanning THz probe tip and also bundled for a THz area emitter.

4. Conclusion

In summary, we report a simple method of making an optical fiber emit terahertz waves. We have devised and demonstrated an optical-fiber THz emitter using a (100)-oriented InAs thin fiim placed on a 45-degree wedged optical fiber tip. The THz wave generation mechanism from the optical fiber tip is explained by the photo-Dember effect in a relatively low band gap semiconductor. In a proof-of-concept experiment using the alignment-free THz source for THz-TDS and THz imaging, we obtained a bandwidth of 2 THz and sub-wavelength spatial resolution. This spatial resolution is measured as 180 μm, three times the size the optical fiber core. Using this method, the THz imaging resolution is expected to be improved to the size of the optical fiber core. The designed compact THz emission tip here can be extended to

#127512 - $15.00 USD Received 27 Apr 2010; revised 6 Jun 2010; accepted 7 Jun 2010; published 10 Jun 2010

near-field imaging, spectroscopy, polarization studies, and remote sensing with sub-wavelength resolution.

Acknowledgments

This work was supported in part by the IT R&D program of MKE/KEIT [2008-F-021-01], and in part by Basic Science Research Program through the National Research Foundation of Korea [No. 2009-0083512]. YDJ acknowledges the support from the Bio-Imaging Research Center and "Fusion-Tech. Developments for THz info. and Comm." program of GIST in 2010.

#127512 - $15.00 USD Received 27 Apr 2010; revised 6 Jun 2010; accepted 7 Jun 2010; published 10 Jun 2010